Rare Metal Materials and Engineering
Volume 46, Issue 11, November 2017
Online English edition of the Chinese language journal

Available online at www.sciencedirect.com
ScienceDirect

Cite this article as: Rare Metal Materials and Engineering, 2017, 46(11): 3228-3232.

ARTICLE

Effect of Deposition Temperature on Structural and Optical Properties of Zno Films Based on Tourmaline Substrates

Zhang Qinghuang, Guo Yun, Xu Jiwei, Wu Ting, Wang Linjun

Shanghai University, Shanghai 200444, China

Abstract: ZnO nanosheet thin films were obtained by the ultrasonic spray pyrolysis technique (USP) on tourmaline and glass substrates at different deposition temperatures. Structural studies show that ZnO crystals are polycrystalline with hexagonal wurtzite structure. The intensity of the characteristic Raman peak, and the (002) preferential orientation, the degree of crystallinity, the grain size achieved by the XRD results are significantly increased with the elevation of the substrate temperature. SEM images show that the ZnO nanoplates laminate parallel to the substrate and assemble to the flower-like column morphology, and ZnO nano crystals have larger lamellae sizes and wider crystalline columns at higher temperature. UV-Vis measurement confirms the maximum absorption peak of the ZnO films on the tourmalines have more red shifts and stronger intensities than that on the glass substrates, and relatively greater wavelength shifts under higher substrate temperature are also observed.

Key words: ZnO; tourmaline; SEM; XRD; Raman; UV-Vis

As a kind of wide band gap semiconductor material, zinc oxide (ZnO) has excellent performances in optics, piezoelectricity and electromechanical coupling properties, free requirements for substrate material, facile synthesis into films, and so on. Thus ZnO material has been playing important roles in the surface acoustic wave, transparent electrodes, blue light devices, gas sensors, etc[1-3]. Nano-crystalline ZnO is well known for its abundant micro-structures, including one-dimensional, two-dimensional and some sophisticated cases which can modulate their multi-functional uses[4-6]. Meanwhile, the option of substrate material acts as a crucial factor for precipitating ZnO film. Over the last decades, different candidates including Si, Al_2O_3, GaAs and SiC etc, had been applied as the geometrical supports for ZnO growth[7-10]. However, the research related to the tourmaline substrate has rarely been reported previously.

Tourmaline is a type of silicate mineral material, with the trigonal system structure, thermoelectricity, piezoelectricity and spontaneous polarization federatively [11]. This polarization effect contributes to its electrostatic field around tourmaline crystals, leading to the extensive applications in electro-magnetic shield, infrared radiation, release of negative ions, so tourmaline crystal has already turned into a natural functional material with far-ranging concerns[12]. The structural characteristics and functional properties of tourmaline, are rather similar to that of ZnO material. Under this circumstances, taking tourmaline crystal as substrates to deposite ZnO film should be a promising attempt, the spontaneous polarization and the intrinsic surface electric field of tourmaline should be beneficial to the ZnO growth, so as to enhance the physical properties and broaden the optoelectronic applications of ZnO-based material.

1 Experiment

Zinc acetate dihydrate ($Zn(Ac)_2$ $2H_2O$) from Sinopharm Chemical Reagent Co., Ltd. was employed to prepare $Zn(Ac)_2$ solution as the precursor solution, with the concentration of 0.1 mol/L at room temperature. The tourmaline crystals from Xinjiang province (XJ) were selected to be as the substrate material comparatively with the glasses slides. Tourmaline was cut into slices with the surface area of 10 mm×10 mm and the thickness of 2 mm parallel to the *C* axis. Then the surface

Received date: November 15, 2016
Foundation item: National Natural Science Foundation of China (113775112)
Corresponding author: Guo Yun, Ph. D., Associate Professor, School of Materials Science and Engineering, Shanghai University, Shanghai 200444, P. R. China, Tel: 0086-21-66135330, E-mail: guoyun@shu.edu.cn

was polished and pre-washed by alcohol and deionized water. 408A ultrasonic nebulizer was used with the fog amount of 4 mL/min and Nitrogen (N_2) was used as the carrier gas with the flow rate of 1.5 L/min. The substrates were put on the heating stage at 300 ℃ and pre-heated for 20 min, the deposition temperature were devised to be 300, 400 and 500 ℃, and the deposition time was set to 60 min. Then the samples were annealed at 580 ℃ in air atmosphere for 70 min with the heating rate of 100 ℃/h, and were cooled down to room temperature naturally.

The sample group of ZnO films on tourmaline and glass substrates were labeled as BL/ZnO and XJ/ZnO, and recorded as BL300, BL400, BL500 and XJ300, XJ400, XJ500 respectively corresponding to the different growth temperatures.

XRD (D/max-111C, Cu target radiation) and Raman (Jobin-YvonHR800, laser wavelength 532 nm) examination were carried out for the structure analysis of ZnO thin films. The surface morphology and UV-Vis optical property research were accomplished by Phillips XL-30ESEM and Ocean Optics GEM-3000.

2 Results and Discussion

2.1 Structural characteristics

The Raman spectra of BL/ZnO and XJ/ZnO films are shown in Fig.1, the strongest peak of the vibration of two groups of samples located at about 435 cm^{-1}, corresponding to the E_2 characteristic vibration mode of hexagonal ZnO. As the substrate temperature rises, the vibration intensity increases. Raman peaks near the 328 and 380 cm^{-1} are assigned to $2E_2$ and A_{1T} vibration modes while the peak at about 581 cm^{-1} interrelating to the lattice defects of the zinc interstitial (O_i) and oxygen vacancy (V_O), belonging to E_{1L} vibration mode [13]. At higher heating temperature for the deposition substrates, the lattice vibration peaks are strengthened together with that of the crystal defect peaks.

Fig.2 shows the XRD patterns of BL/ZnO and XJ/ZnO. Two sets of samples present significantly three strong diffraction peaks of Z(100), Z(002), and Z(101) between the 2θ degree form 30°~40°, which can be well indexed to the typically hexagonal wurtzite structure of ZnO crystal (JCPDS card No. 36-1451) [14].

The structural parameters analysis of ZnO thin films are given in Table 1 as below, including the full width at half maximum (FWHM), the mean grain size (nm), and the dependence of texture coefficient (TC).

The FWHM data were derived from the prime diffraction plane of (002) peak. The average crystallite size of the ZnO films was calculated using the classical Scherrer formula. Herein, the texture coefficient TC (*hkl*) was given by

$$TC = \frac{I(hkl)/I_0(hkl)}{\sum I(hkl)/I_0(hkl)} \quad (1)$$

Where $I(hkl)$ iss the measured relative intensity of a crystal plane (*hkl*), and $I_0(hkl)$ is the standard intensity of the crystal plane taken from the JCPDS data[15].

From Table 1, firstly, the FWHM of (002) peak of BL/ZnO and XJ/ZnO obviously declines with the increasing of the substrate temperature, which approve the crystallinity of the

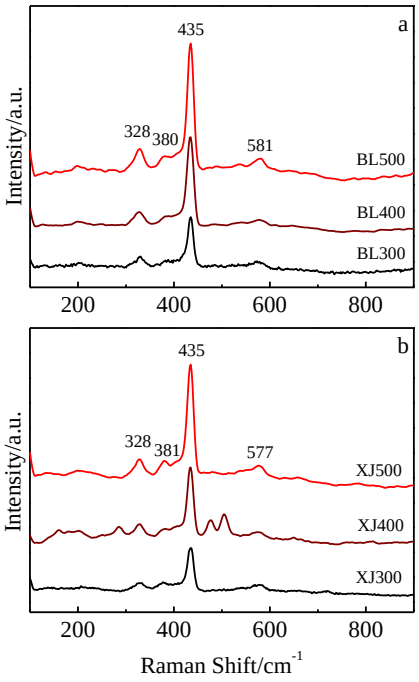

Fig.1 Raman spectra of ZnO films on glass and tourmaline substrates: (a) BL/ZnO and (b) XJ/ZnO

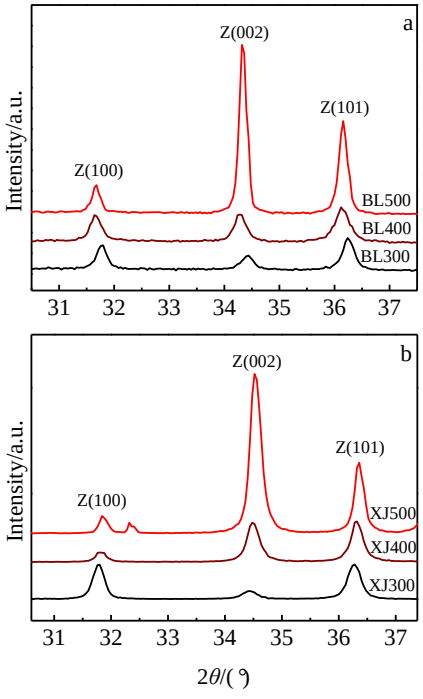

Fig.2 XRD patterns of ZnO on glass and tourmaline substrates: (a) BL/ZnO and (b) XJ/ZnO

Table 1 Structural parameters of ZnO from XRD analysis

Sample group	Samples	(002) FWHM/(°)	Particle size/nm	TC (*hkl*) of (100)/(002)/(101)/%
BL/ZnO	BL300	0.215	43.7	0.398/0.305/0.297
	BL400	0.209	45.4	0.306/0.462/0.232
	BL500	0.172	59.2	0.084/0.760/0.156
XJ/ZnO	XJ300	0.304	29.0	0.538/0.158/0.304
	XJ400	0.268	33.5	0.114/0.623/0.262
	XJ500	0.239	38.4	0.060/0.799/0.141

ZnO crystals have accordingly improved, since the FWHM data has been an effective indicator for investigating the material crystallinity. At the same temperature, the FWHM of BL/ZnO is smaller than that of XJ/ZnO and represen- tative of a better crystallization property.

Secondly, when the substrate temperature are 300, 400 and 500 ℃, the crystal particle sizes of BL/ZnO and XJ/ZnO are theoretically calculated as 43.7, 45.4, 59.2 nm and 29.0, 33.5, 38.4 nm, respectively, which reveals that the increase of the substrate temperature have made all of the ZnO crystal grains get coarser unexceptionally. Meanwhile, the grain sizes of XJ/ZnO series are contrastively smaller, which should be correlated to the inhibition effect on the ZnO growth by virtue of the tourmaline spontaneous polarization[16]. The finer crystal particles would bring about lager specific surface area and contribute to the applications in gas sensitivity and photo catalysis etc.

Thirdly, whereas in common, ZnO crystal has an advan- tageous growth direction along *C*-axis, while the data of Texture Coefficient (TC) can be used to describe the preferential growth direction[17]. As shown in Table 1, the TC (hkl) data has obviously shifted from TC (100) under 300 ℃ to TC (002) under 400 and 500 ℃ on both sets of substrates, which indicates that ZnO crystals have more advantageous growth along *C*-axis at higher temperature. Furthermore, as the same temperature concerns, the TC values of BL/ZnO are smaller than that of XJ/ZnO may be related to the surface electrical field of tourmaline crystal, which act more effectively on the oriented arrangment along *C*-axis especially at higher substrate temperature.

2.2 Surface morphology characteristics

The surface morphological characteristics of ZnO films were investigated by SEM explorations (at high magnification of 40 000×), in which, Fig.3a~3c are for the BL/ZnO series and Fig.3d~3f are for the XJ/ZnO series.

It is clear that, from Fig.3a to 3c in the series of glass substrates, the ZnO products present as the flower-like crystal column appearance perpendicular to the substrates, and the crystalline column's width is about 1 μm. As the deposition temperature increases, the crystal width has gradually enlarged. In the inner part of the flower-shaped crystalline columns, ZnO single crystal is defined into nearly hexagonal platelets with the thickness of nanometer scale. The crystalline plates are stacking layer by layer along the *C*-axis to assemble into the flower-like morphology in parallel with the substrate direction.

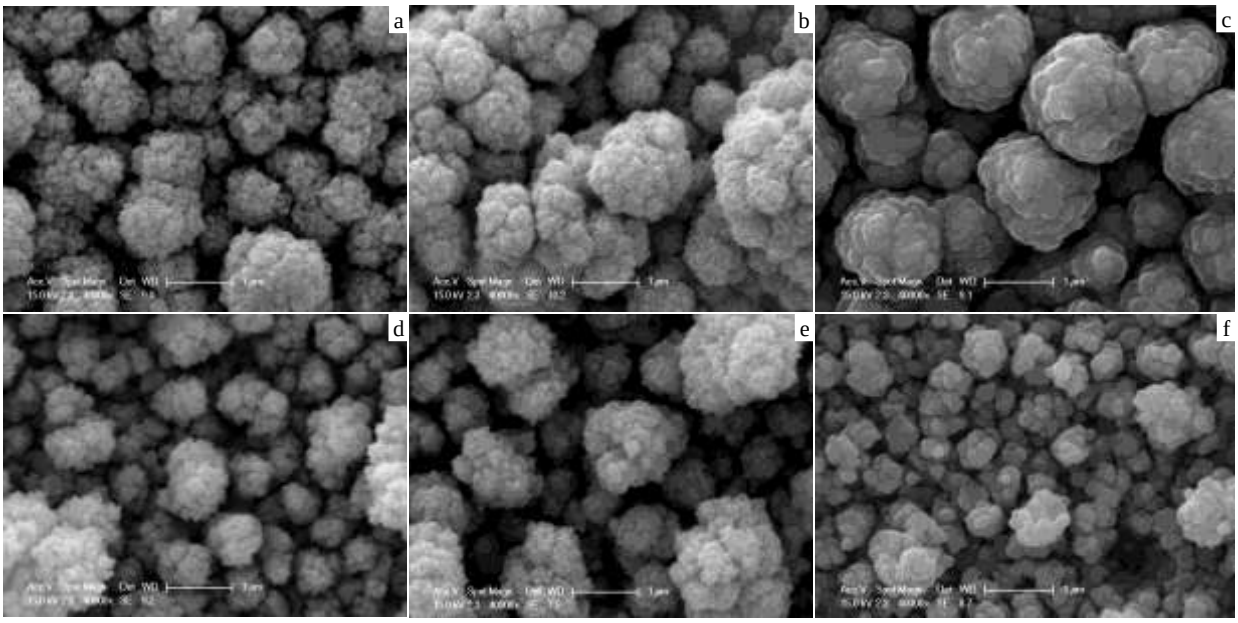

Fig.3 SEM images of glass and tourmaline substrates: (a) BL300, (b) BL400, (c) BL500, (d) XJ300, (e) XJ400, and (f) XJ500

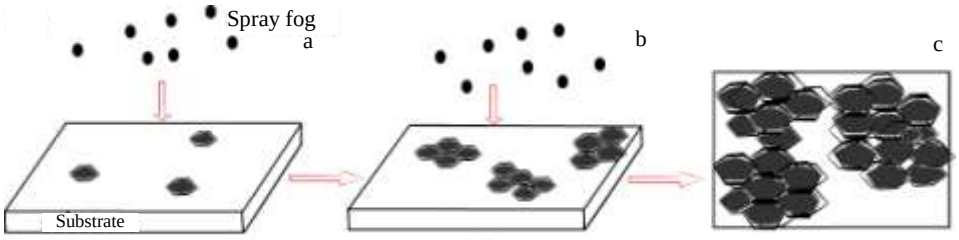

Fig.4 Schematic diagram for the formation of ZnO morphology: (a) ZnO nano-sheets formed on the substrates, (b) ZnO nanoplates assembled to nanoflower, and (c) flower-like columns from the top view

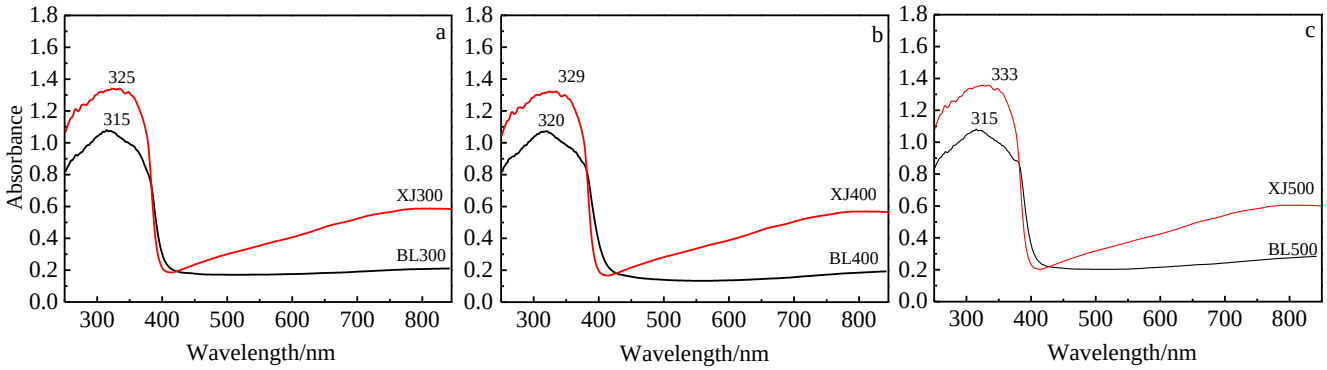

Fig.5 UV-Vis curves of ZnO on glass and tourmaline substrates at different temperatures: (a) 300 ℃, (b) 400 ℃, and (c) 500 ℃

Similarly in the tourmaline substrate cases from Fig.3d to 3f, ZnO nano-plates also laminate into flower-like crystalline columns vertically to the substrate, but the general sizes of the crystalline lamellae and columns shrink due to the surface electrical field effect as we studied in the XRD analysis. And it also could be seen that, ZnO crystals show better crystallinity, more perfect configuration, and more structured arrangement at higher deposition temperature.

Based on the above observations, a reasonable formation process of ZnO thin films are shown in Fig.4a~4c, which are in accordance with the growth mode of the nanoplate-nanoflower - nanocolumn, as Fig.4c is specially shown from the top view.

2.3 UV-Vis Analysis

Fig.5 shows the UV-Vis absorption curves of BL/ZnO and XJ/ZnO. As we could see, the main absorption edges of ZnO are located between 350~360 nm.

To different substrate materials, there are certain improvements in the maximum absorption peak (MAP) intensity of XJ/ZnO in comparison to that of BL/ZnO, which are from 1.10± to 1.35±, and the MAP wavelength of XJ/ZnO are all red-shifted. In general cases, due to the grain boundary effects of polycrystalline thin films, the electric field formed by the charges and the barriers at the grain boundaries would cause the band gap of the semiconductor material to become wider, and the absorption band will move towards the shorter wavelength [18]. However herein, the surface electric field of the tourmaline substrate may have some absorptance action to the boundary charges, so as to counteract the electric field at the interface of the ZnO particles, which result in the red-shifted characteristic of the MAP. The higher the substrate temperature is, especially in the XJ/ZnO product series, the greater the wavelength red shift which is correlated to the stronger polarization intensity of tourmaline crystal and the coarser particles of ZnO crystals as we discussed in XRD structural parameters mentioned above.

3 Conclusions

1) The as-prepared crystal are wurtzite polycrystalline structure with greater intensity of Raman characteristic peaks at 435 cm^{-1} and more preferential orientation along (002) plane; simultaneously, better crystallinity and bigger-sized grains have been achieved at higher substrate temperature. Nearly hexagonal platelets of ZnO nano-crystals stack along the direction parallelling the substrate and crystal into flowery micro-columns.

2) As the substrate temperature increases, ZnO nanosheets and the crystalline columns become wider. Comparing with the UV-Vis absorption spectra, the maximum absorption peak (MAP) intensity in XJ/ZnO increases to 1.35 while that is 1.10 in BL/ZnO. Due to the effective counteraction for the grain boundary charges by the surface electric field effect of tourmaline substrate, the absorptance of ZnO presents red shifts, with relatively greater wavelength shifts at higher heating temperature.

3) Under different deposition temperature conditions,

selecting tourmaline slices as the substrate materials can have regulatory effects on the ZnO crystal structures and growth morphologies, and exert certain influences on the photoelectric properties for nano-crystalline ZnO thin films, for instance, on the optical absorption characteristics in this contribution.

References

1 Özgür Ü, AlivovY, Liu C *et al*. *Journal of Applied Physics*[J], 2005, 98 (4): 1

2 Min J H, Wang B, Liang X Y *et al*. *Rare Metal Materials and Engineering*[J], 2011, 40(5): 761 (in Chinese)

3 Gu X Q, Qiang Y H, Zhao Y L *et al*. *Rare Metal Materials and Engineering*[J], 2014, 43(6): 1296 (in Chinese)

4 Choi S, Shim D S, Jung S H *et al*. *Materials Letters*[J], 2009, 63(8): 739

5 Zhang J J, Guo E J, Wang L P *et al*. *Transactions of Nonferrous Metals Society of China*[J], 2014, 24: 736

6 Yan L, Li G Z, Zou Y L *et al*. *Transactions of Nonferrous Metal Society of China*[J], 2014, 24(9): 2896

7 Cheng J P, Zhang X B, Luo Z Q *et al*. *Surface and Coatings Technology*[J], 2008, 202(19): 4681

8 Zhao B J, Yang H J, Du G T *et al*. *Journal of Crystal Growth*[J], 2003, 258(1-2): 130

9 Cui Y G, Zhang Y T, Zhu H C *et al*. *Journal of Crystal Growth*[J], 2005, 282(3-4): 389

10 Sun B, Li R P, Zhao C Y *et al*. *Journal of Inorganic Materials*[J], 2008, 23(4): 753 (in Chinese)

11 Yamaguchi S. *Applied Physics A*[J], 1983, 31(4): 183

12 Zhan J, Hao X P, Liu H *et al*. *Journal of Functional Materials*[J], 2006, 37(4): 524 (in Chinese)

13 Zhao L L, Wang J Y, Li J *et al*. *Journal of the Chinese Ceramic Society*[J], 2012, 40(12): 1773 (in Chinese)

14 Sun Y L, Bian J M, Li Q W *et al*. *Journal of Inorganic Materials*[J], 2010, 25(10): 1115 (in Chinese)

15 Mahajan C M, Takwale M G. *Journal of Alloys and Compounds*[J], 2014, 584: 128

16 Wang H Q, Li C H, Zhao H G *et al*. *Advanced Powder Technology*[J], 2013, 24: 599

17 Guo Y, Xia Y B, Min J H *et al*. *Journal of Inorganic Materials*[J], 2010, 25(7): 717 (in Chinese)

18 Zhang S C, Li C H, Li X G. *Acta Physico-Chimica Sinica*[J], 2004, 20: 902

基于电气石衬底的沉积温度对 ZnO 薄膜结晶和光学特性的影响

张清煌，郭　昀，徐积维，吴　婷，王林军

(上海大学，上海 200444)

摘　要：利用超声雾化热解技术 (USP) 在不同温度的电气石和玻璃衬底上生长 ZnO 纳米片状薄膜。结构研究表明晶体为六方纤锌矿多晶结构。衬底温度越高，Raman 特征峰越强，XRD 结果给出（002）优势定向越明显，晶体结晶性能越好，晶粒尺寸越大。SEM 图像显示片状 ZnO 晶体沿平行衬底方向叠加形成花状晶柱的微观形貌，沉积温度越高，晶柱宽度越大。UV-Vis 表明电气石衬底上 ZnO 吸收峰强度高于玻璃衬底，最大吸收峰位置发生红移，高温下移动更大。

关键词：ZnO；电气石；SEM；XRD；Raman；UV-Vis

作者简介：张清煌，男，1989 年生，硕士生，上海大学材料科学与工程学院，上海 200444，E-mail: zhangqinghuang@shu.edu.cn